Electronic Supplementary Material (ESI) for New Journal of Chemistry.
This journal is © The Royal Society of Chemistry and the Centre National de la Recherche Scientifique 2024

Supporting information

Novel porphyrin-based donor-acceptor conjugated organic polymers for efficient photocatalytic production of hydrogen peroxide in pure water

Renbao Zhang[a,1], Hui Zhao[a,1], Chengsi Pan[a], Jiawei Zhang[a], Liang Jian[a], Xinyu Sun[a], Rong Ji[a], Jiawei Li[a], Yuming Dong[a,*], and Yongfa Zhu[b]

[a]*International Joint Research Center for Photoresponsive Molecules and Materials, Key Laboratory of Synthetic and Biological Colloids, School of Chemical and Material Engineering, Jiangnan University, Wuxi 214122, China.*

[b]*Department of Chemistry, Tsinghua University, Beijing 100084, China*.

[1]*These authors contributed equally: Renbao Zhang, Hui Zhao.*

[*]e-mail: *dongym @jiangnan.edu.cn*

1. Test Methods

1.1. Determination of H_2O_2 concentration

The concentration of H_2O_2 was determined using the traditional titanium potassium oxalate titration method and the absorption peak measured was 400 nm. Preparation of titanium potassium oxalate solution: 1.77 g of titanium potassium oxalate, 12 mL of concentrated sulfuric acid, formulated into a 250mL solution, which was fixed in a 250 mL volumetric flask. Pipette 3 ml of the solution to be measured with a pipette gun, transfer it to 2 ml of potassium titanium oxalate solution, let it stand for 5 min, and measure it with a UV-Vis spectrophotometer.

1.2. Photochemical decomposition of H_2O_2 on materials

The decomposition of H_2O_2 was carried out by dispersing the catalyst (10 mg) in an aqueous solution (20 mL) containing H_2O_2 (0.8 mM) under Ar atmosphere. Visible light irradiation ($\lambda > 420$ nm) was achieved using a cut-off filter with a 300 W Xe lamp as a light source. The concentration of H_2O_2 was measured as described above.

1.3. Solar-to-chemical energy conversion (SCC) efficiency

Photocatalytic experiments simulating solar irradiation (A.M 1.5G, 100 mW cm^{-2}) were realized using a 300 W Xe lamp as a light source and a cut-off filter to determine the SCC efficiency. The catalyst (160 mg) and water (40 mL) were placed in a sealed device consisting mainly of quartz tubes and sealing components, and O_2 was continuously energized for 1 h of light irradiation.

$$\text{SCC efficiency}(\%) = \frac{\left[\Delta G\ for\ H_2O_2\ generation(Jmol^{-1})\right][H_2O_2\ formed(mol)]}{[Total\ input\ power(W)][Reaction\ time(s)]} \times 100\%$$

Where ΔG=117 kJmol^{-1}。

1.4. Apparent quantum yield (AQY) measurements

The apparent quantum yield (AQY) was measured under irradiation with 300 W Xe lamps with different bandpass filters ($\lambda_0 \pm 20$ nm) for 1 h. Catalyst (160 mg) and water (40 mL) were placed in a sealed unit consisting primarily of quartz tubes and sealing components and continuously passed through O_2. The average irradiation intensity was determined to be 10.0 mW·cm^{-2} by means of an ILT 950 spectroradiometer and the irradiated area was controlled to be 3.14 cm^2.

$$\text{N(mol)} = \frac{E}{h\nu}$$

$$\text{AQY}(\%) = \frac{\left[H_2O_2\ generated(mol)\right] \times 2}{N} \times 100\%$$

1.5. Rotating disk electrode (RDE) measurements

The rotating disk electrode (RDE) was tested in O_2 saturated phosphate buffer (0.1 M, pH=6.9), with the disk electrode as the working electrode, the platinum ring as the counter electrode, and the Ag/AgCl electrode as the reference electrode. The

working electrode was prepared by dispersing the photocatalyst (5 mg) in ethanol (1 ml) containing Nafion (50 μL), and then the mixture (20 μL) to the disk electrode and dried at room temperature. Linear scanning voltammetry (LSV) tests were performed at a scanning speed of 10 $mV \cdot S^{-1}$ and at different rotational speeds. The average number of electrons (n) was calculated from the Koutecky-Levich equation:

$$\frac{1}{J} = \frac{1}{J_L} + \frac{1}{J_K} = \frac{1}{B\omega^{1/2}} + \frac{1}{J_K}$$

$$B = 0.2nFC_0D_0^{2/3}\nu^{-1/6}$$

where J is the measured current density, ω is the angular velocity, n is the number of transferred electrons, F is the Faraday's constant (96485 $C \cdot mol^{-1}$), C_0 is the volumetric concentration of O_2 (1.26×10^{-6} $mol \cdot cm^{-3}$), D_0 is the diffusion coefficient of O_2 in 0.1 M phosphate buffer solution (2.7×10^{-5} $cm^2 \cdot s^{-1}$), and ν is the kinetic viscosity of the electrolyte (0.01 $cm^2 \cdot s^{-1}$).

1.6. Nitroblue tetrazolium (NBT) method for the detection of $\cdot O_2^-$

NBT method: 10 mg of catalyst was dispersed in 20 ml of aqueous NBT solution at a concentration of 2.0×10^{-5} M. The temperature was controlled at 25 °C by circulating water, and then irradiated under a light source of a 300 W xenon lamp (equipped with a cut 420 nm filter). Prior to irradiation, the suspension was exposed to O_2 for 10 min in the dark, and after irradiation, samples were taken at specific times, 2 ml at a time. The photocatalytic production of $\cdot O_2^-$ was determined by the degradation of NBT and was detected by absorbance at a wavelength of 259 nm. The molar ratio of generated $\cdot O_2^-$ to degraded NBT was 4:1.

1.7. Electron spin resonance (ESR) experimental steps

The ESR was tested using the EMXplus-10/12 (Brooklyn, Germany). Before testing, 2 ml of methanol solution with a catalyst concentration of 0.5 mg/mL was first prepared. Then the original DMPO solution was diluted 10 times. Before illumination, 20 μL of the diluted DMPO solution was added to 200 μL of the material dispersion, mixed well, and subjected to free radical testing under dark conditions. The above mixture was then placed under a xenon lamp light source for 10 min for free radical testing under light.

1.8. In-situ DRIFTS Characterization

In situ Fourier transform infrared (in situ FT-IR) spectroscopic measurements were performed using a Nicolet iS50 spectrometer (Thermo, USA). Samples were first prepared by dispersing 5 mg of catalyst in 2 ml of ethanol solution containing 50 μL of Nafion resin. The silicon crystals were then polished and sanded to make the surface smooth. Next, 20 μL of the suspension was evenly dripped onto the surface of the silicon crystals and dried under an infrared lamp. Finally, an appropriate amount of aqueous solution was added to the reaction cell, connected to an IR instrument, and tested under continuous O_2 passages.

2. Supporting information

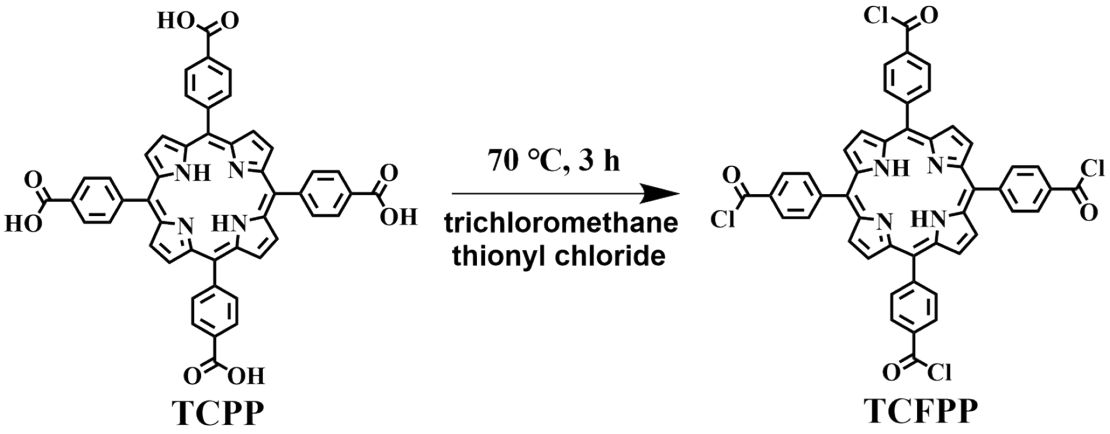

Figure S1: Schematic of TCFPP synthesis.

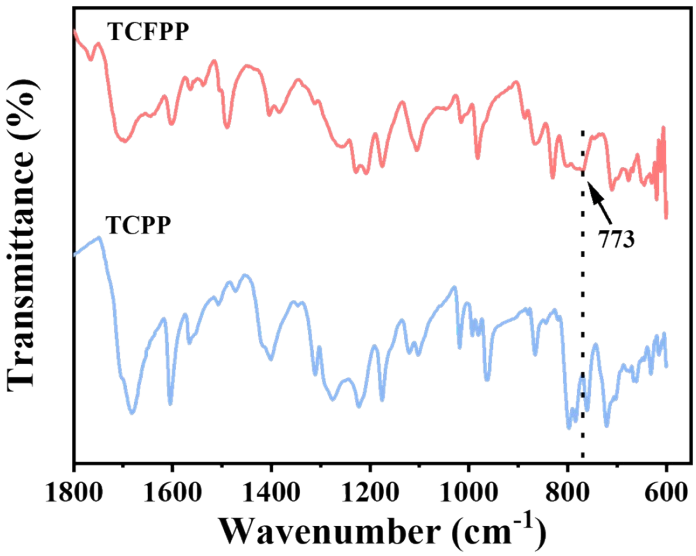

Figure S2：FT-IR spectra of TCPP and TCFPP.

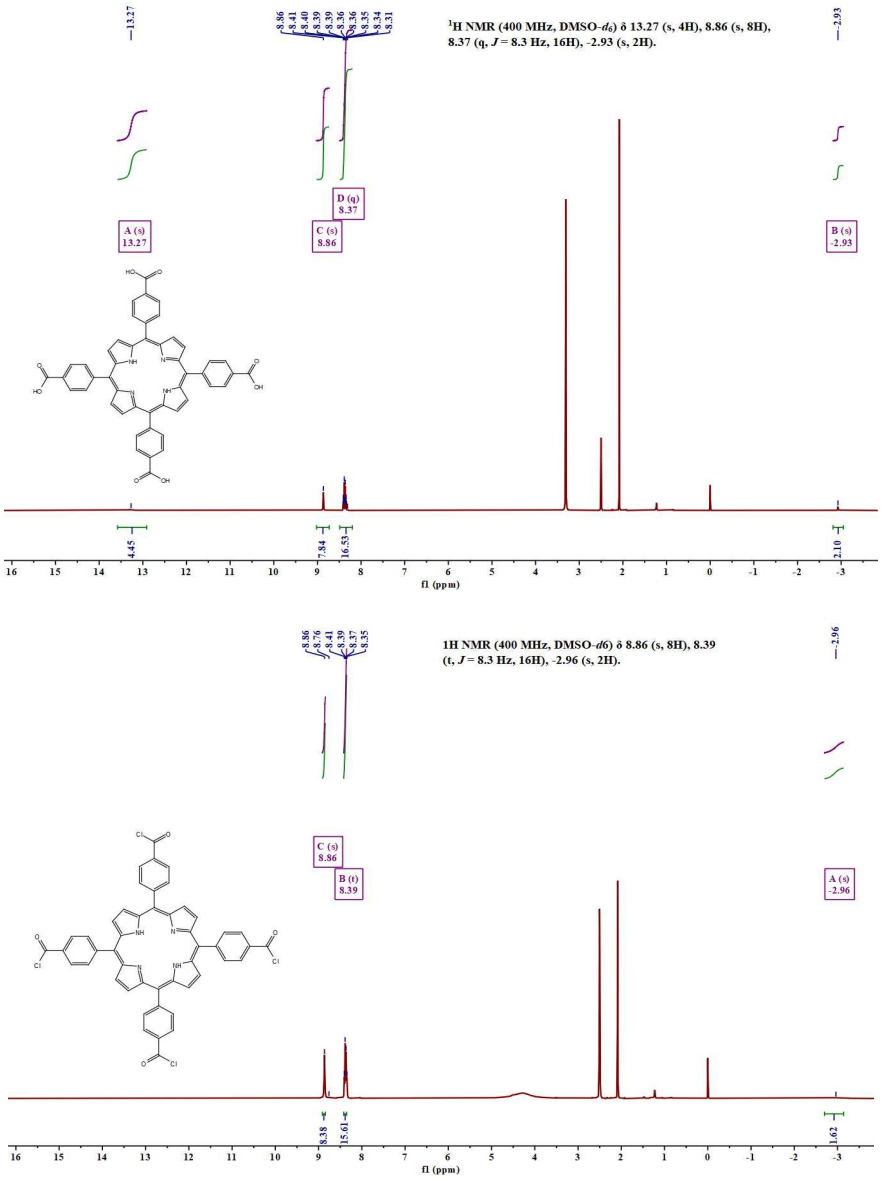

Figure S3: ^{1}H NMR of TCPP and TCFPP.

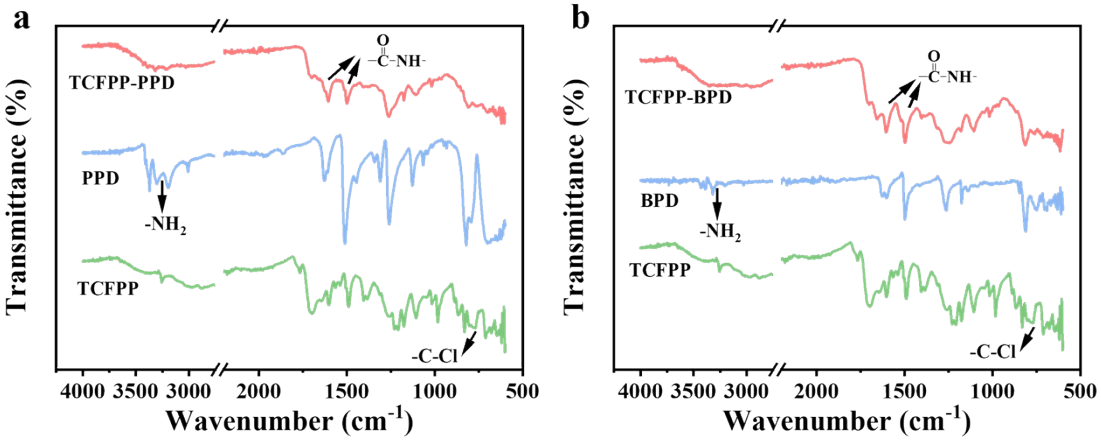

Figure S4: FT-IR spectra of (a) TCFPP-PPD and (b) TCFPP-BPD.

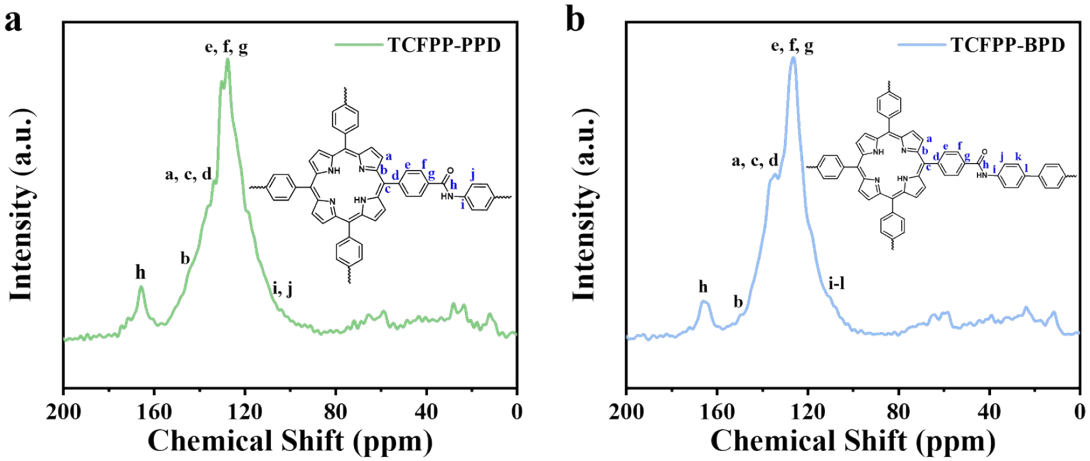

Figure S5: ^{13}C solid-state NMR spectra of (a) TCFPP-PPD, (b) TCFPP-BPD.

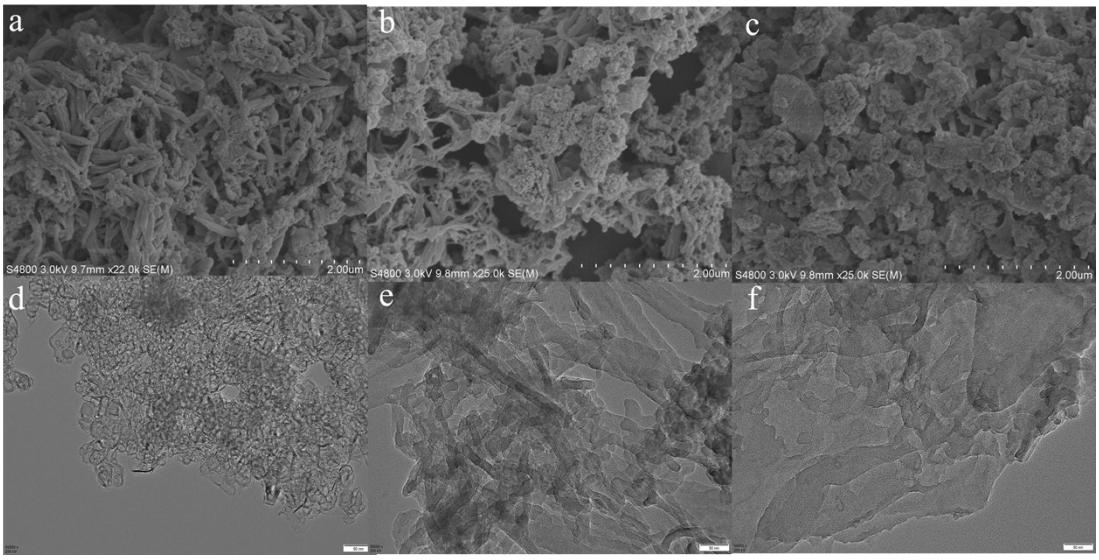

Figure S6: SEM (a), (b) , (c) and TEM (d), (e) , (f) images of TCFPP-PPD, TCFPP-BPD and TCFPP-TPD.

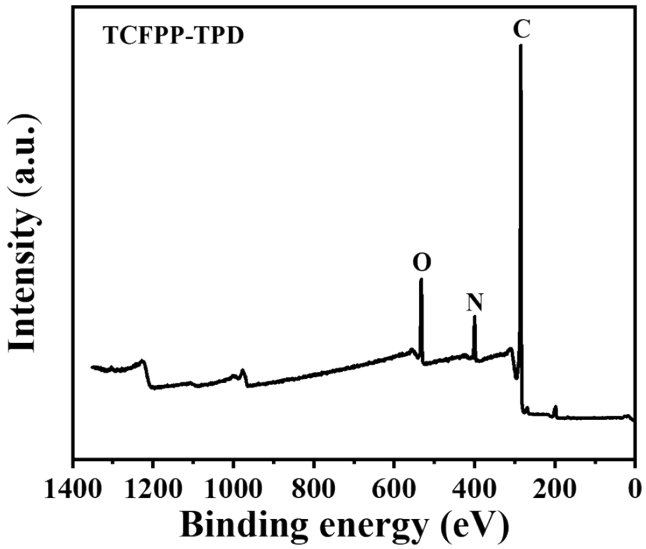

Figure S7: XPS total spectrum of TCFPP-TPD.

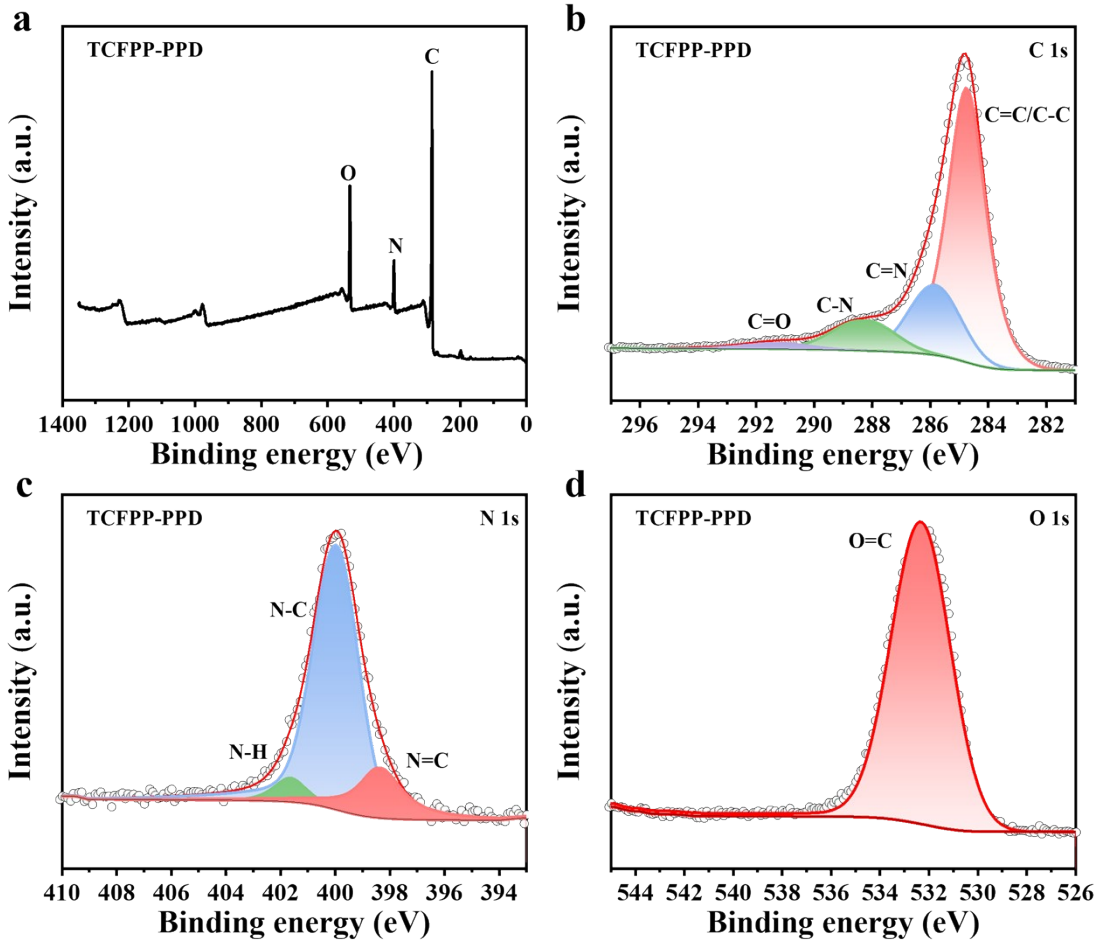

Figure S8: XPS profiles of TCFPP-PPD: (a) total spectrum; (b) C 1s; (c) N 1s; (d) O 1s.

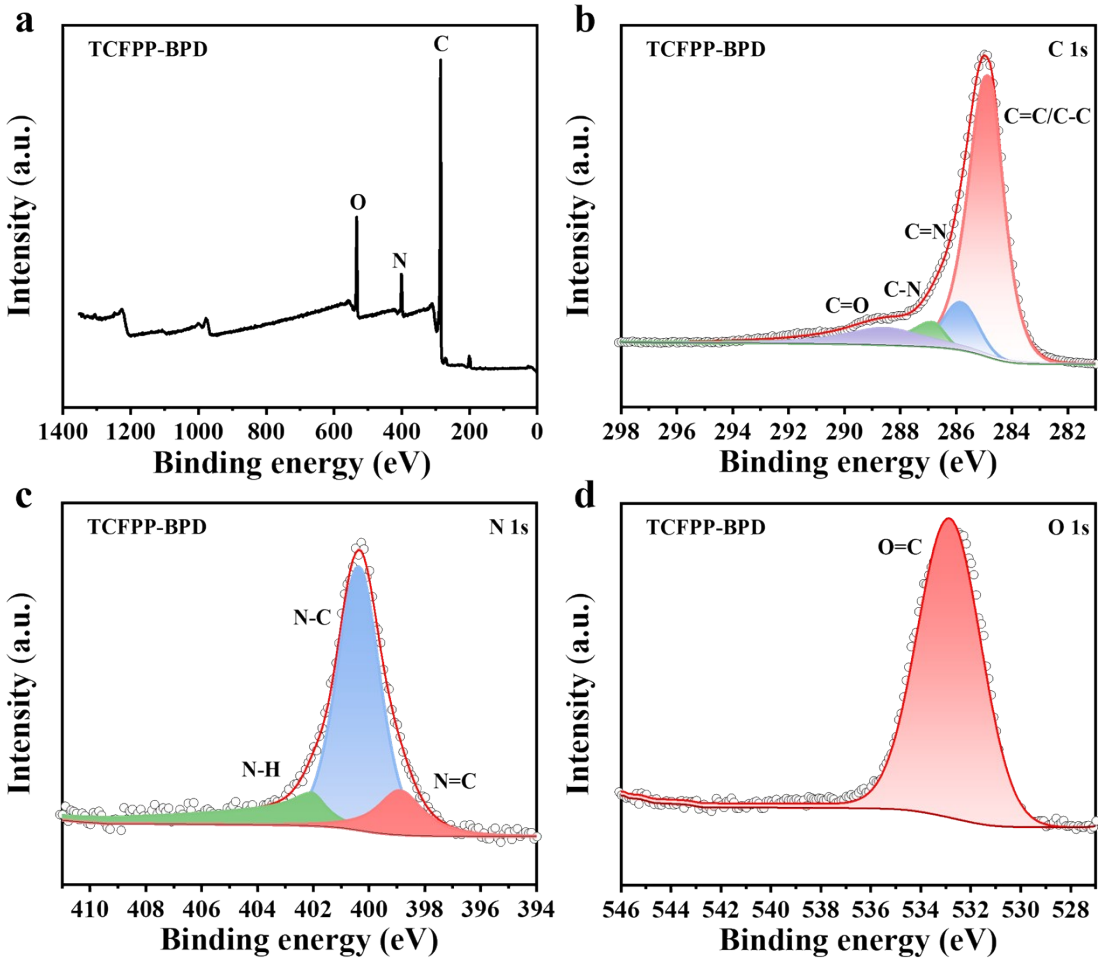

Figure S9: XPS profiles of TCFPP-BPD: (a) total spectrum; (b) C 1s; (c) N 1s; (d) O 1s.

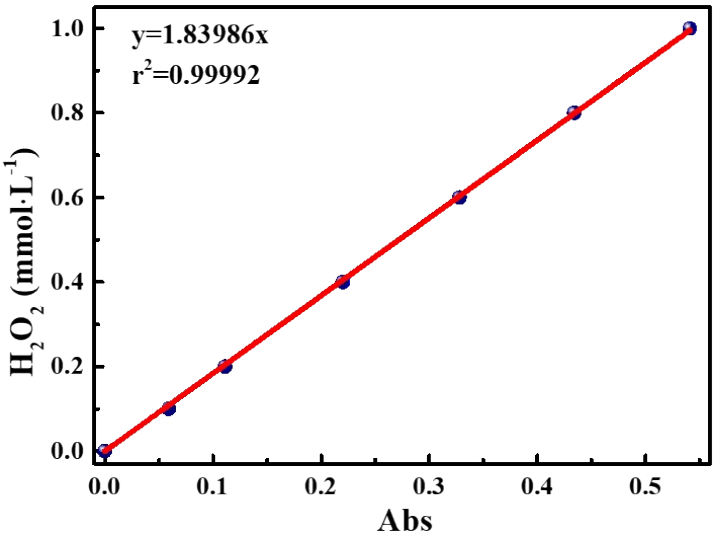

Figure S10: Fitted curve of UV-visible absorbance with H_2O_2 concentration.

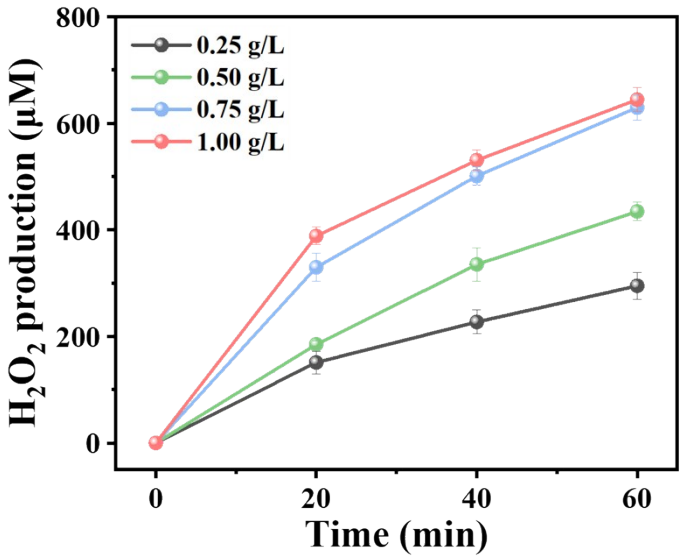

Figure S11: H_2O_2 production at different concentrations of TCFPP-TPD.

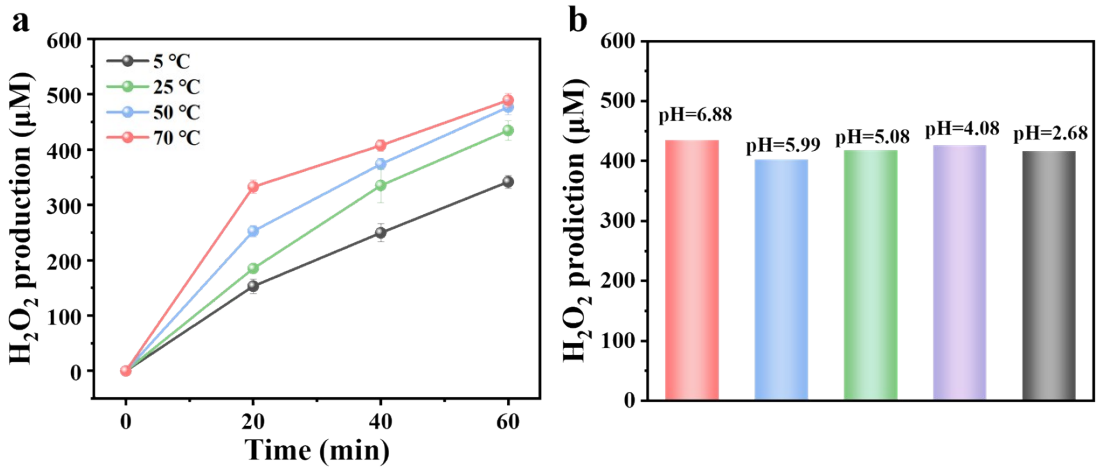

Figure S12: H_2O_2 yield of TCFPP-TPD under different conditions (a) temperature; (b) pH.

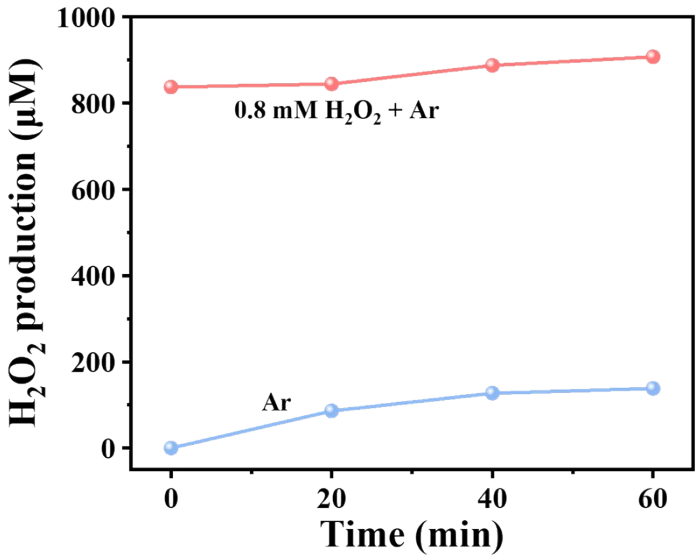

Figure S13: Decomposition of H_2O_2 on the TCFPP-TPD surface.

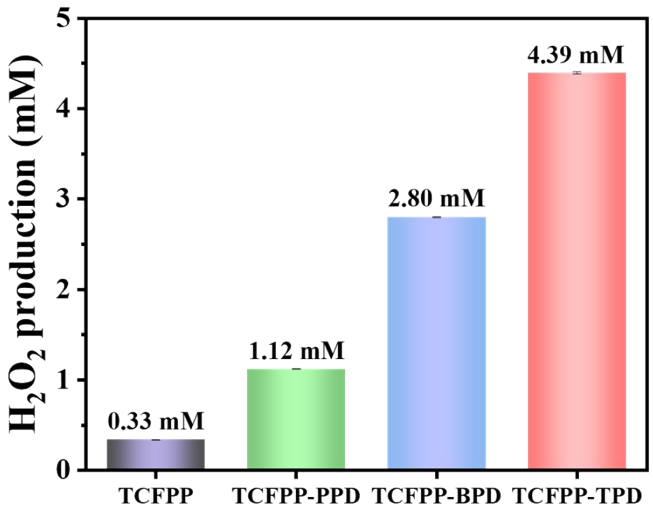

Figure S14: Histograms of the long time cumulative performance of TCFPP, TCFPP-PPD, TCFPP-BPD and TCFPP-TPD.

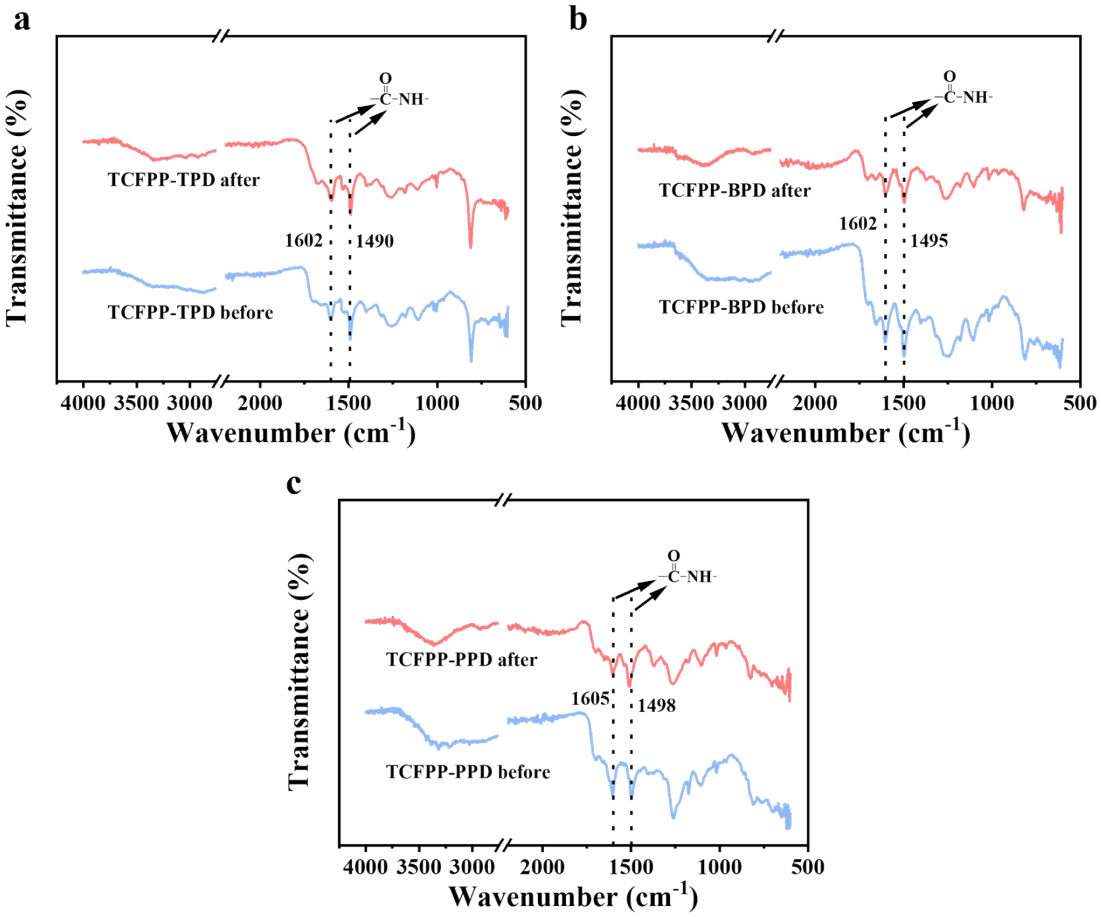

Figure S15: FT-IR before and after the reaction of (a) TCFPP-TPD, (b) TCFPP-BPD and (c) TCFPP-PPD.

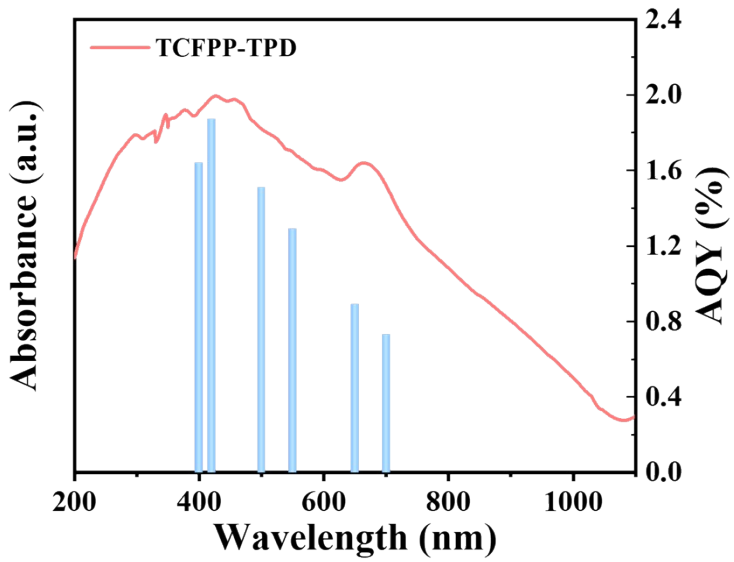

Figure S16: AQY of TCFPP-TPD at different single optical wavelengths.

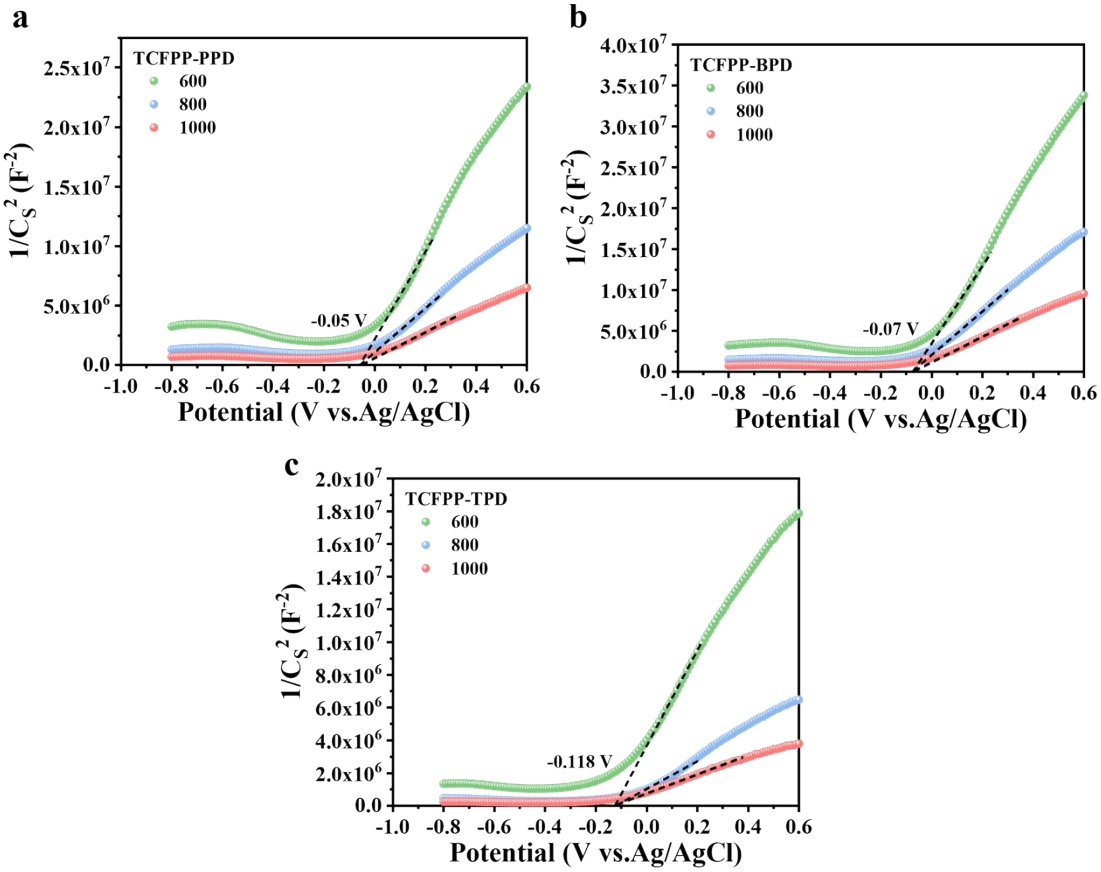

Figure S17: Mott mapping of (a) TCFPP-PPD, (b) TCFPP-BPD and (c) TCFPP-TPD.

The band edge positions of catalysts can be calculated using the following equation:

$$E_{CB}\,(V\ vs.\ NHE) = E_{fb}(V\ vs.\ AgCl/Ag) + 0.197 - X \text{------Eq. s1}$$

$$E_{VB} = E_{CB} + E_g \text{----- Eq. s2}$$

Where E_{VB} and E_{cB} stand for the valence band edge potential and conduction band edge potential, respectively; X is the voltage difference between the conduction band value and the flat potential value, generally 0.1-0.3 eV (the conduction bands of n-type semiconductors are normally 0.1-0.3 eV deeper than the flat-band potential). Therefore, the conduction band position is obtained by subtracting 0.2 eV from the potential of each flat band.

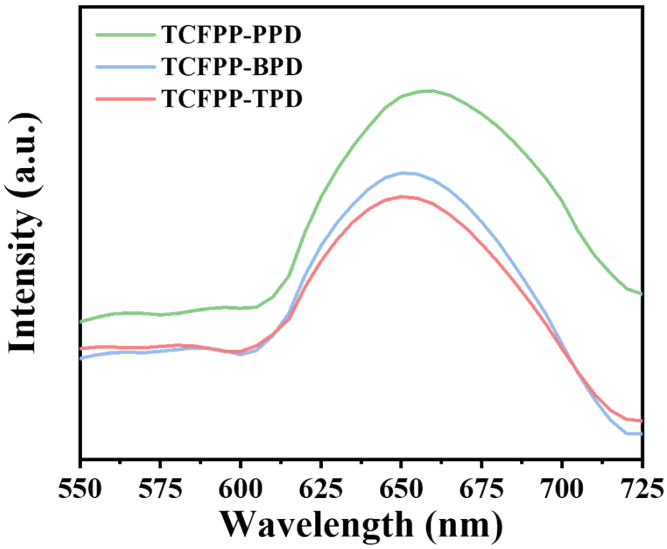

Figure S18: PL mapping of TCFPP-PPD, TCFPP-BPD and TCFPP-TPD.

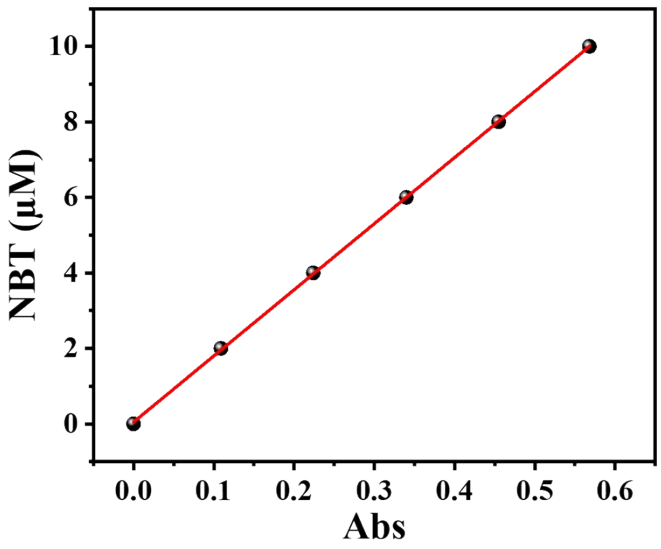

Figure S19: Fitted curve of UV-visible absorbance with NBT concentration.

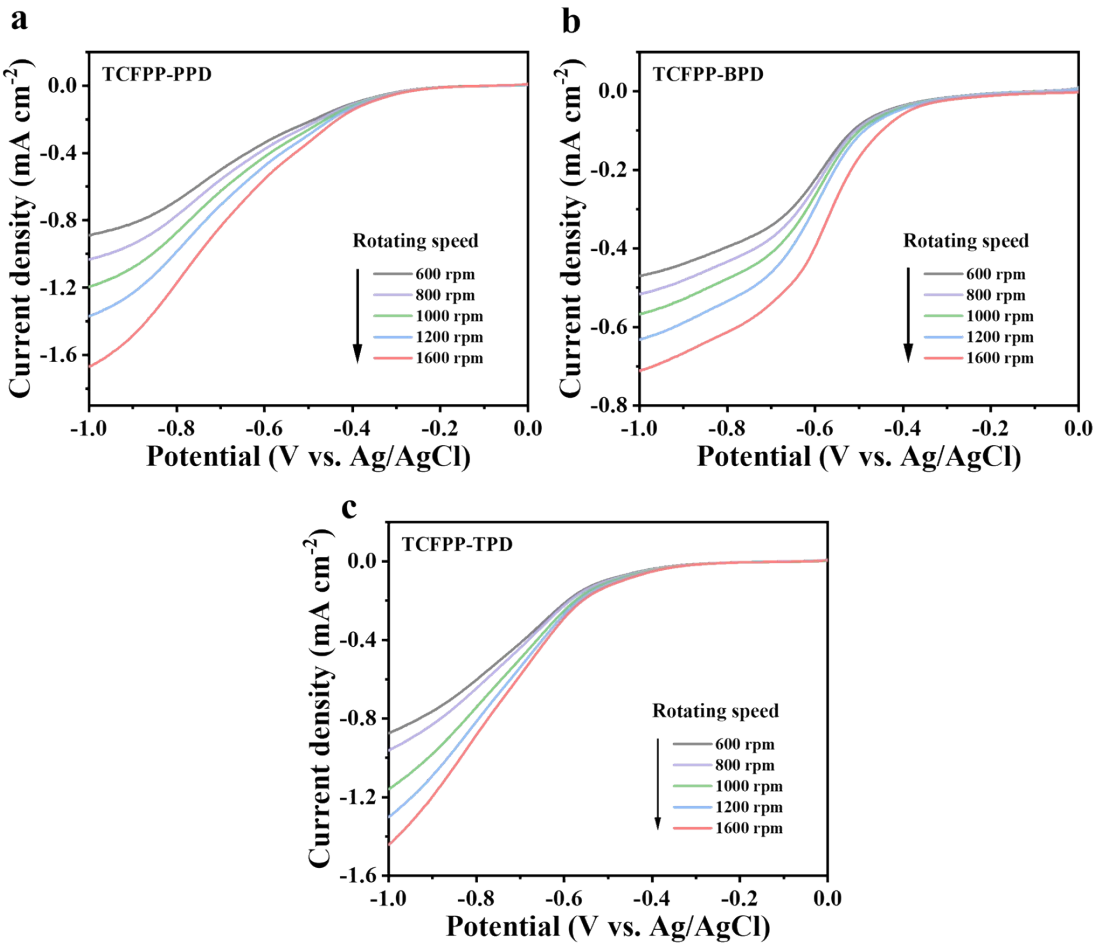

Figure S20: Linear scanning RDE voltammograms of (a) TCFPP-PPD, (b) TCFPP-BPD and (c) TCFPP-TPD.

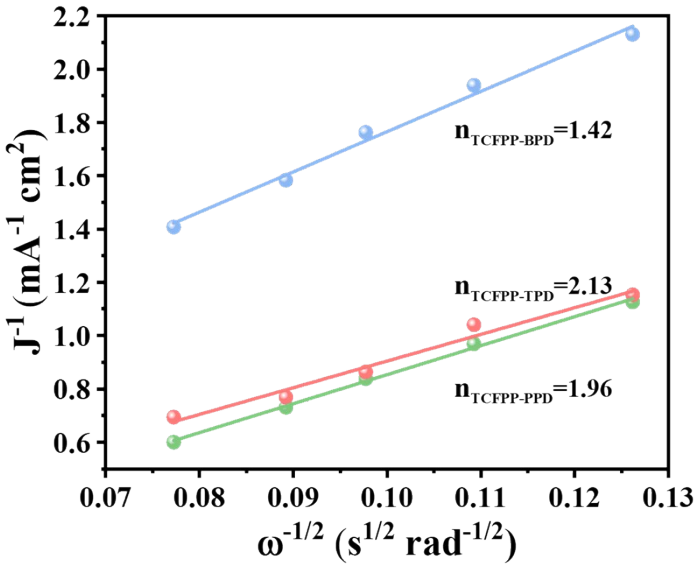

Figure S21: Koutecky-Levich diagram obtained from RDE measurements.

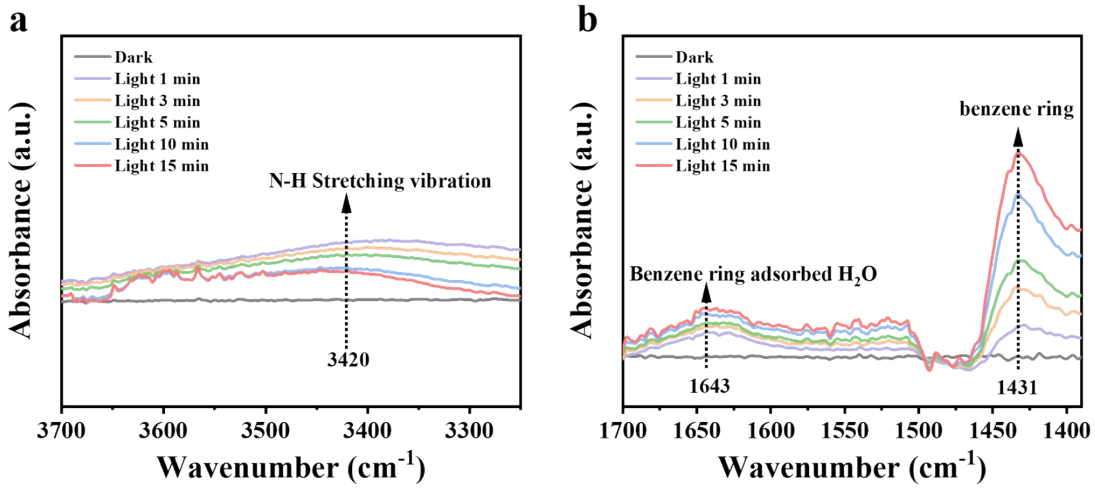

Figure S22: In situ FT-IR of TCFPP-TPD (a) 3700 cm^{-1}-3250 cm^{-1}; (b) 1700 cm^{-1}-1390 cm^{-1}.

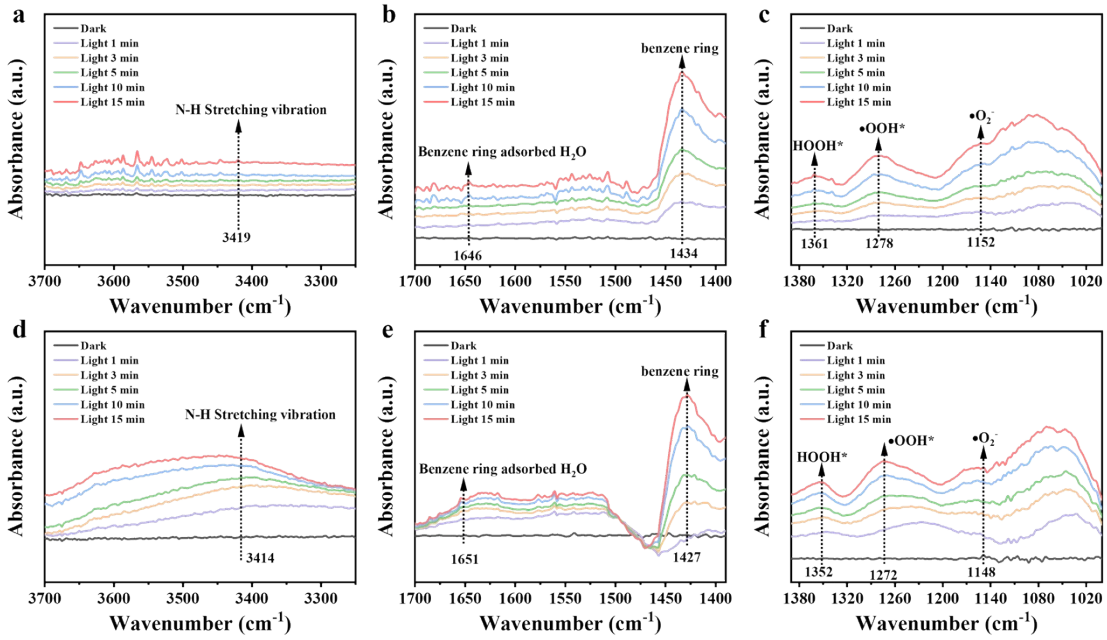

Figure S23: In situ FT-IR of TCFPP-PPD (a) 3700 cm^{-1}-3250 cm^{-1}; (b) 1700 cm^{-1}-1390 cm^{-1}; (c) 1390 cm^{-1}-1000 cm^{-1}; In situ FT-IR of TCFPP-BPD (d) 3700 cm^{-1}-3250 cm^{-1}; (e) 1700 cm^{-1}-1390 cm^{-1}; and (f) 1390 cm^{-1}-1000 cm^{-1}.

Table S1: Comparison of H_2O_2 production from polymer photocatalytic materials.

Photocatalyst	**H_2O_2 yield rate/ μmol·g^{-1}·h^{-1}**	**Irradiated conditions**	**Solvent**	**AQY**	**Ref**
RF-523	51.7 μmol·g^{-1}·h^{-1}	λ> 420 nm	H_2O	8% (420 nm)	1
PEI/C_3N_4	208.1 μmol·g^{-1}·h^{-1}	AM 1.5	H_2O	2.1% (420 nm)	2
TAPD-$(Me)_2$COF	234.52 μmol·g^{-1}·h^{-1}	λ> 420 nm	H_2O:EtOH (1:9)	N.A	3
OCN-500	106 μmol·g^{-1}·h^{-1}	λ> 420 nm	H_2O	10.2% (420 nm)	4
DE7-M	2200 μmol·g^{-1}·h^{-1}	λ> 300 nm	H_2O	8.7% (420 nm)	5
CHF-DPDA	256 μmol·g^{-1}·h^{-1}	λ> 420 nm	H_2O	16% (420 nm)	6
EBA-COF	1830 μmol·g^{-1}·h^{-1}	λ> 420 nm	H_2O:EA(9:1)	4.4% (420 nm)	7
COF-TfpBpy	1042 μmol·g^{-1}·h^{-1}	λ> 420 nm	H_2O	8.1% (420 nm)	8
TDB-COF	723.5 μmol·g^{-1}·h^{-1}	AM 1.5	H_2O	1.4% (365 nm)	9
TaptBtt	1407 μmol·g^{-1}·h^{-1}	λ> 420 nm	H_2O	4.6% (450 nm)	10
TCFPP-TPD	1180 μmol·g^{-1}·h^{-1}	λ> 420 nm	H_2O	1.87% (420 nm)	**This work**

References

1. Y. Shiraishi, T. Takii, T. Hagi, S. Mori, Y. Kofuji, Y. Kitagawa, S. Tanaka, S. Ichikawa and T. Hirai, *Nature Materials* **2019**, *18*, 985-993.
2. X. Zeng, Y. Liu, Y. Kang, Q. Li, Y. Xia, Y. Zhu, H. Hou, M. H. Uddin, T. R. Gengenbach, D. Xia, C. Sun, D. T. McCarthy, A. Deletic, J. Yu and X. Zhang, *ACS Catalysis* **2020**, *10*, 3697-3706.
3. C. Krishnaraj, H. Sekhar Jena, L. Bourda, A. Laemont, P. Pachfule, J. Roeser, C. V. Chandran, S. Borgmans, S. M. J. Rogge, K. Leus, C. V. Stevens, J. A. Martens, V. Van Speybroeck, E. Breynaert, A. Thomas and P. Van Der Voort, *Journal of the American Chemical Society* **2020**, *142*, 20107-20116.
4. Z. Wei, M. Liu, Z. Zhang, W. Yao, H. Tan and Y. Zhu, *Energy & Environmental Science* **2018**, *11*, 2581-2589.
5. L. Liu, M.-Y. Gao, H. Yang, X. Wang, X. Li and A. I. Cooper, *Journal of the American Chemical Society* **2021**, *143*, 19287-19293.
6. H. Cheng, H. Lv, J. Cheng, L. Wang, X. Wu and H. Xu, *Advanced Materials* **2022**, *34*, 2107480.
7. L. Zhai, Z. Xie, C.-X. Cui, X. Yang, Q. Xu, X. Ke, M. Liu, L.-B. Qu, X. Chen and L. Mi, *Chemistry of Materials* **2022**, *34*, 5232-5240.
8. M. Kou, Y. Wang, Y. Xu, L. Ye, Y. Huang, B. Jia, H. Li, J. Ren, Y. Deng, J. Chen, Y. Zhou, K. Lei, L. Wang, W. Liu, H. Huang and T. Ma, *Angewandte Chemie International Edition* **2022**, *61*, e202200413.
9. Z. Zhou, M. Sun, Y. Zhu, P. Li, Y. Zhang, M. Wang and Y. Shen, *Applied Catalysis B: Environmental* **2023**, *334*, 122862.
10. C. Qin, X. Wu, L. Tang, X. Chen, M. Li, Y. Mou, B. Su, S. Wang, C. Feng, J. Liu, X. Yuan, Y. Zhao and H. Wang, *Nature Communications* **2023**, *14*, 5238.